Green Chemistry

PAPER

View Article Online
View Journal | View Issue

Cite this: *Green Chem.*, 2016, **18**, 5594

Compositional and structural feedstock requirements of a liquid phase cellulose-to-naphtha process in a carbon- and hydrogen-neutral biorefinery context†

A. Deneyer,[a] T. Ennaert,[a] G. Cavents,[a] J. Dijkmans,[a] J. Vanneste,[a,b] C. M. Courtin,[c] M. Dusselier*[a] and B. F. Sels*[a]

Processing raw (ligno)cellulosic feedstock into renewable light naphtha alkanes could lead to a gradual replacement of fossil feedstock for the production of chemicals, materials and fuels. The production of drop-in alkanes is a preferable short term strategy because of its practical implementation and integration in existing infrastructure and processes. A handful of promising cellulose-to-alkane biorefinery initiatives were recently reported, both processing in gas and liquid phase. This contribution presents a detailed study of the two-liquid phase hydrodeoxygenation of cellulose to *n*-hexane under relatively mild circumstances, proceeding through the recently communicated HMF route, in presence of a soluble acid and Ru/C metal catalyst. Two main points were addressed here: (i) the importance (or not) of the lignocellulose pretreatment and purification to the alkane yield, and (ii) the renewability of the consumed hydrogen in the process. A systematic study of the effect of cellulose purity, crystallinity, degree of polymerization and particle size (surface area) on the light naphtha yield was performed to tackle the first part. As fibrous cellulose with large particles was the most favourable feedstock with regard to alkane yield and as the presence of hemicellulose and lignin impurities had no effect on the cellulose-to-naphtha conversion, costly mechanical and purification steps are redundant to the process, in contrast to their notable importance in other cellulose valorisation processes (*e.g.* to glucose, sorbitol, isosorbide and acids). The second point regarding sustainable hydrogen supply is discussed in detail by calculating hydrogen and carbon mass and energy balances of the chemical conversions, assuming selected scenarios among others to recuperate the hydrogen by steam-reforming of waste streams (like gaseous $C_{<6}$ hydrocarbons and aqueous polyol fractions) and (partial) aromatization of the C_6 fraction into benzene. The study shows potential to integrate the liquid phase cellulose-to-naptha (LPCtoN) technology into a self-sufficient biorefinery, in which the chemical processes may run without consumption of external (non-renewable) hydrogen, carbon and energy, except for solar light.

Received 16th June 2016,
Accepted 27th July 2016

DOI: 10.1039/c6gc01644h

www.rsc.org/greenchem

Introduction

Current climate problems, geo-political frictions and the exhausting long term availability of fossil resources require at least a partial transition to renewable alternatives in the chemical industry. Biomass and more specifically lignocellulose may become an important feedstock for the production of chemicals, materials and in some cases (additives for) fuels.[1–14] The carbon skeleton and the high functionality per C-atom offer beautiful possibilities to synthesize novel components and platform molecules.[15–25] Lignocellulose is for instance also a great alternative resource for the production of fossil-based alkanes.[1,6,13] The light naphtha fraction is nowadays an important group of hydrocarbons with a myriad of applications in the chemical industry. Light naphtha reforming for instance leads to the production of high-octane gasoline, which is typically composed of short and branched alkanes,[26] cracking gives ethylene, propylene and butadiene building blocks,[27,28] while selective catalytic cyclization/dehydrogenation produces aromatics.[29–31] One important light

[a]*Center for Surface Chemistry and Catalysis, KU Leuven, Celestijnenlaan 200f, 3001 Heverlee, Belgium. E-mail: michiel.dusselier@kuleuven.be, bert.sels@kuleuven.be*
[b]*Materials Department, Flemish Institute for Technological Research (VITO), Boeretang 200, 2400 Mol, Belgium*
[c]*Center for Food and Microbial Technology, KU Leuven, Kasteelpark Arenberg 22, 3001 Heverlee, Belgium*

†Electronic supplementary information (ESI) available: ESI contains SEM pictures, particle size distributions and PXRD patterns of celluloses, as well as detailed mass and energy balance schemes and calculations. See DOI: 10.1039/c6gc01644h

naphtha compound cyclohexane is oxidized to adipic acid, a nylon precursor.[32,33] Today, a handful of cellulose-to-alkane technologies are presented. Recent thermochemical approaches such as (hydro)pyrolysis are robust technologies producing complex and sometimes unstable product mixtures.[34–43] Mild catalytic liquid phase approaches offer the advantage of better preserving the original C skeleton, for instance by forming *n*-hexane from cellulose. Much work has been reported on the depolymerisation of cellulose into its building blocks and their subsequent conversion to different platform molecules. Hydrodeoxygenation (HDO) of these molecules, with or without C–C coupling, leads to the formation of alkanes.[6,44–52] Recently described one-pot liquid phase cellulose-to-naphtha (LPCtoN) conversion strategies, as depicted in Fig. 1, though promising, are in its infancy and less studied so far.[53–56]

Tomishige *et al.* developed such a one-pot process producing *n*-hexane from cellulose in a biphasic solvent system of water and *n*-dodecane. Hydrolysis of cellulose to glucose takes place in the aqueous phase in presence of HZSM-5 zeolite. The metal catalyst Ir-ReO_x/SiO_2 hydrogenates glucose to sorbitol in the aqueous phase, and subsequent C–O hydrogenolysis cycles forms *n*-hexane. After 24 h, a yield of 78 mol% C hexane (in total of 90% light naphtha alkanes) from microcrystalline cellulose was reached at 483 K.[53] This sorbitol pathway was also investigated using a Ru/C catalyst combined with $LiNbMoO_6$ in aqueous phosphoric acid yielding 72 mol% C of C_6 alkanes after 24 h at 503 K. The layered structure of the catalysts is said to inhibit the formation of (too stable) isosorbide.[54]

Alternatively to the sorbitol pathway, there is the 5-hydroxymethylfurfural (HMF) pathway, as recently introduced by Op de Beeck *et al.*[55] The combination of a soluble tungstate acid and a modified Ru/C in a biphasic water–alkane environment stimulates glucose dehydration to HMF and its further hydrogenation, while retarding direct sugar hydrogenation to sorbitol. The authors assumed that Ru sintering, altered through modification, favors the HMF pathway. To corroborate this hypothesis, characterization and differences in activity between a typical Ru/C and the modified Ru/C (htTSA(2)Ru/C) were reported in the manuscript of Op de Beeck *et al.*[55] Consecutive dehydration and hydrogenation cycles from HMF ultimately lead to the production of alkanes from microcrystalline cellulose (Avicel PH-101), yielding 42 mol% C of hexane (of a total of 60 mol% C light naphtha alkanes) within 3 h at 493 K. Other components in the organic phase are mostly oxygenates, such as (di)methyltetrahydrofuran, oxepane, (methyl-)tetrahydropuran and hexanols. The aqueous phase consists of isosorbide and sorbitan isomers.

Though promising, these cellulose-to-alkane technologies require more intense research. The atom and energy efficiency of the conversion of preferentially raw cellulose is essential herein.[57] To bridge the gap between model and real cellulosic feedstock, this paper attempts to map the influence of the cellulose characteristics like purity, particle size (surface area), degree of polymerization and crystallinity on its conversion to light naphtha for the HMF route technology. A second part attempts the development of reaction (process) schemes to realize closed energy and mass balances for the LPCtoN biorefinery, suggesting several strategies to recuperate hydrogen from product and waste streams. While the latter goal is essential in light of devising an overall carbon and hydrogen neutral

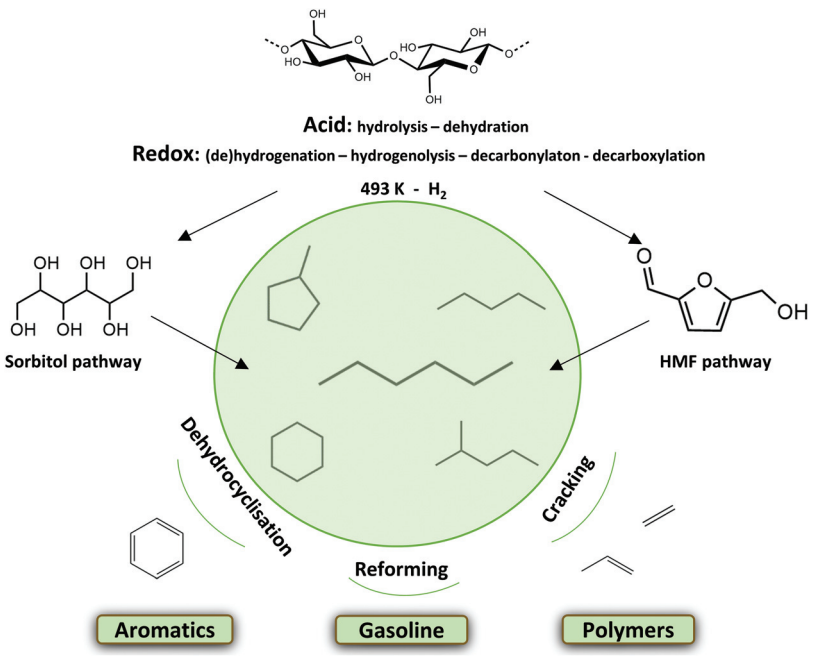

Fig. 1 Mild catalytic conversion of cellulose to light naphtha *via* two reaction pathways, through sorbitol or HMF, and their subsequent valorisation.

process, the first objective will assess the requirement (or not) of (costly) feedstock pretreatment.

Experimental

For a list of all used chemicals and materials as well as a more additional description of the experimental procedures, the reader is referred to the ESI.†

For the pretreatment, a Ru/C (5 wt%) metal catalyst is modified in a 100 ml batch reactor (Parr Instrument Co.). The reactor is typically loaded with Ru/C (1 g), TSA hydrate (0.25 g) and water (40 ml). After flushing with N_2, the reactor was pressurized with a H_2 pressure of 50 bar at room temperature. Subsequently, a stirring rate of 700 rpm was installed. A temperature program, starting at room temperature to 483 K (±10 K min^{-1}) and staying for 1 h at 483 K, is followed. Finally, the synthesized catalyst (htTSA(2)Ru/C) was filtered, washed with water until neutral pH of the effluent and dried to constant weight.

Catalytic conversion of various cellulose substrates (2 g) was carried out in a 100 ml batch reactor (Parr Instrument Co.). In addition, a biphasic system water : *n*-decane (30 : 10 ml), TSA hydrate (4.8 g) and htTSA(2)Ru/C (0.25 g) was loaded into the reactor. After flushing with N_2, the reactor was pressurized at 50 bar of hydrogen and room temperature. Subsequently, a stirring rate of 700 rpm was installed. A temperature program, going from room temperature to 423 K (±12 K min^{-1}) and further to 493 K (±0.5 K min^{-1}), is followed. After a reaction of 5 h, the reactor is cooled, depressurized and opened for sampling and analysis. Products yields are expressed as mol% C and mostly presented with just % in the results section.

$$\text{Yield}(\text{mol\% C}) = \frac{\text{moles C in product}}{\text{moles C in feedstock}} \times 100$$

Cellulose powders were characterized by different techniques: FTIR, PXRD, laser diffraction, SEM and viscosimetry. FTIR spectra were recorded by using a Bruker IFS 66v/S instrument (KBr method). Crystallinity (CrI%) was recorded with powder X-ray diffractions (PXRD) patterns at room temperature on a STOE STADI P Combi diffractometer. The diffracted intensity of the CuKα radiation (λ = 0.154 nm) was measured in a 2θ range between 0° and 62.5°. Crystallinity based on PXRD was determined with the peak height method.[58] Particle sizes (μm) were determined by laser diffraction with a Microtrac S 3500. To remove all particles from earlier measurements, the machine was first flushed with air. After measuring some blanks, powders were systematically sucked for 10 s towards the cell where particles were measured with a TRI-LASER multi-detection system. Data handling was done with Microtrac flex 11.0.0.3 software. SEM pictures were recorded by using a JEOL JSM-6010 JV microscope after coating the samples with gold with a JEOL JSC-1300 sputter. Viscosimetry based on the NF G 06-037 norm was used to measure the degree of polymerization (DP). Typically, 0.125 g (or 0.015 g when a high DP was expected) cellulose was dissolved in 50 ml of a 0.5 M cuprietethylenediamine solution and stirred for 2 hours at room temperature. Viscosity data were determined in a UBBELOHDE thermostated capillary tube viscosimeter at 298 K and afterwards calculated according to the NF G 06-037 norm.

The thermodynamics of the proposed processes were calculated under common process conditions (with regard to temperature and pressure) by using Aspen Tech 7.3 software. The process streams were based on stoichiometric relations after equalizing the amount of H_2 in the entire process. The mass and energy balances are calculated taking into account a stand-alone biorefinery for *n*-hexane and benzene production, which is self-sufficient in hydrogen and energy.

Results and discussion

Influence of cellulose properties

A systematic study on the LPCtoN conversion was initially performed with common pure cellulose powders, *viz.* commercial Avicel PH-101 and various Sigmacell celluloses as well as with unusual substrates such as Vivapur, Whatman filters and cotton. The different cellulose feedstocks with their physical characteristics and the corresponding alkane yield after the cellulose-to-naphtha catalytic processing are summarized in Table 1. Vivapur cellulose proved to be structurally similar to Avicel, but with bigger particle sizes (Table 1, entry 8). Whatman filters (Fig. S1 in ESI,† FTIR spectra), which are manufactured from cotton, and cotton itself are characterized by a high degree of polymerization in comparison with the other cellulose substrates (Table 1, entries 11–14, viscosimetry). SEM pictures show a fibrous, highly dense structure for the filter material, whereas the classic cellulose powders consist of aggregated particles/spheres (Fig. S2 in ESI†).

The influence of crystallinity is systematically investigated first by prior ball-milling of microcrystalline Avicel at various contact times.[59] After an initial drop, the particle sizes stay more or less constant with the milling time (Table 1, entries 1–4). This treatment creates amorphous regions especially when the milling time is high.[60] Surprisingly, cellulose amorphization has no influence on the cellulose-to-naphtha efficiency. The second property of this series, *i.e.* the degree of polymerization (DP, expressed in # glucose units per chain), which drops by milling, is thus also an unimportant parameter to the alkane yield.

In contrast to crystallinity and degree of polymerization, the effect of particle size (diameter in μm, laser diffractometry) seems more pronounced: indeed, larger particles result in substantially higher light naphtha yields, as seen slightly for the Avicel samples (*e.g.* compare entry 1 with 2), but more clear in the Sigmacell series (compare entries 5 and 6, with similar DP and crystallinity). To confirm the hypothesis, Vivapur cellulose, which comprises of large particles, is tested before and after sieving it into two size fractions (entries 8–10). The Vivapur fraction with particles above 125 μm has a three-times average particle size compared to the small-particle fraction according

Table 1 HDO of different pure cellulose substrates[a]

			Properties[c]			Yield (%)			
Entry	Type cellulose	Pretreatment	Particle size (μm)	Crystallinity (CrI%)	DP (# units)	*n*-Pen	*n*-Hex	Other alkanes[b]	Light naphtha
1	Avicel PH-101	None	68	79	161	7	46	9	62
2		Ball-milling 0.5 h	56	53	149	8	43	7	58
3		Ball-milling 2 h	56	<5	137	9	43	8	60
4		Ball-milling 6 h	57	<5	116	8	46	8	62
5	Sigmacell Type 20	None	29	76	168	8	41	7	56
6	Sigmacell Type 50	None	97	80	165	8	48	10	66
7	Sigmacell Type 101	None	16	48	442	5	38	7	50
8	Vivapur	None	204	78	170	10	48	9	67
9		Sieving: <125 μm	93	74	179	8	45	9	62
10		Sieving: >125 μm	291	80	170	10	51	9	70
11	Whatman filter 1	None	n.d.r.	69	1125	10	46	9	65
12	Whatman filter 4	None	n.d.r.	65	685	10	49	10	69
13	Whatman filter 5	None	n.d.r.	60	729	10	47	9	66
14	Cotton	None	n.d.r.	64	1141	15	48	9	72

[a] Conditions: 2 g cellulose; 4.8 g TSA; 0.25 g htTSA(2)Ru/C; biphasic system: water/*n*-decane (30 : 10); 50 bar H_2 at RT; temperature programme: RT to 423 K (±12 K min^{-1}) and from 423 K to 493 K (±0.5 K min^{-1}); total reaction time of 5 h. Blank reactions with *n*-decane (and squalane) as organic solvent did not give any cracking products. [b] Other alkanes: *n*-butane; 2-methylpentane; 3-methylpentane; methylcyclopentane and cyclohexane. [c] Ennaert *et al.* recently published the properties of certain cellulose substrates (entries 1–7).[23] Characterization data is also available in section B of the ESI. Particle size measurements indicate diameters. n.d.r.: could not be determined reliably (fibrous).

to the particle distribution, as ascertained by laser diffraction (Fig. 2A). Processing the large-particle fraction gives a substantial 10% higher yield of light naphtha in comparison to reaction with the small particle fraction (<125 μm), corresponding to a 13% relative yield increase. Reactions with the other celluloses, of which the results are displayed in Fig. 2E, substantiate the relationship between light naphtha yield and particle size. The figure plots the naphtha yield in function of cellulose particles radius, together with the calculated external surface areas, while assuming spherical particles and constant cellulose densities of 1.5 g cm^{-3} (section C of the ESI†). It is important to notice the rapid decay of surface area, indicating that a small increase in radius for small particles (<30 μm) results in a strong decrease of external surface. Clearly, the naphtha yield increases in a reverse trend with the surface area. This evolution, going from small (Sigmacell Type 101), over medium (Vivapur <125 μm), to very large particles (Vivapur >125 μm) is visualized with the corresponding SEM pictures and laser diffraction data (Fig. 2A–D). Taken together, our observations prove that the particle size, and linked with that, the external surface area of the cellulose particles is the most important substrate parameter, impacting the cellulose-to-naphtha yield. This can be rationalized as follows: as the soluble acid catalyst needs to hydrolyze cellulose at its external surface,[61,62] larger particles infer a more gradual release of the monomeric sugar units to the solution because of its low surface area. In our strongly acidic environment at 493 K, soluble sugars or other reaction intermediates, notably HMF, can lead to side-products such as humins through polymerization[63,64] and this is usually more pronounced at higher sugar concentrations.[65,66] In line with these findings, a higher cellulose loading (here: Sigmacell Type 50, from 5 wt% to 10 wt%) gives a decrease in light naphtha alkanes (from 66% to 42%). Likely, this is due to the higher concentration of glucose and reactive intermediates such as HMF, at a certain moment, causing more degradation products to form. A slower sugar release by hydrolysis (resembling a glucose fed-batch reactor), giving lower concentrations of intermediates, could thus be at the basis of the more efficient conversion of large-sized cellulose to light naphtha. This observation is in stark contrast to most other catalytic cellulose conversion systems, as they preferentially require a more accessible and broken down cellulose structure. This is for instance the case in the LPCtoN process, following the sorbitol pathway. As a heterogeneous acid catalyst was used here, cellulose accessibility is essential, while the sugars are stabilized into hexitols *via* fast hydrogenation.[53] Recently, also Ennaert *et al.* confirmed the need for small and amorphous cellulose particles for the conversion of cellulose into sorbitol.[23] Interestingly, the LPCtoN process following the HMF route has no need to such usually costly (mechanical) feedstock pretreatment.[67–69] The catalytic results of the Whatman filter cellulose and cotton (Table 1, entries 11–14) are in line with the above conclusions: use of dense, fibrous celluloses with high DP show the highest naphtha yields, up to 72% in case of cotton.

Towards real (ligno)cellulosic feedstocks

The pure cellulose model substrates used above, underwent several process cleaning steps, starting from wood and other plant-based products. Usually, raw woody materials consists of 40–50 wt% cellulose, 20–35 wt% hemicellulose and 15–20 wt% lignin.[15] After Kraft pulping, lignin and hemicellulose are (partially) degraded and dissolved, leaving insoluble α-cellulose which is filtered off.[70–72] The α-cellulose consists of cellulose fibers (Fig. S2 in ESI†), that contains small amounts of hemicellulose (17%). Organosolv is another technology to isolate

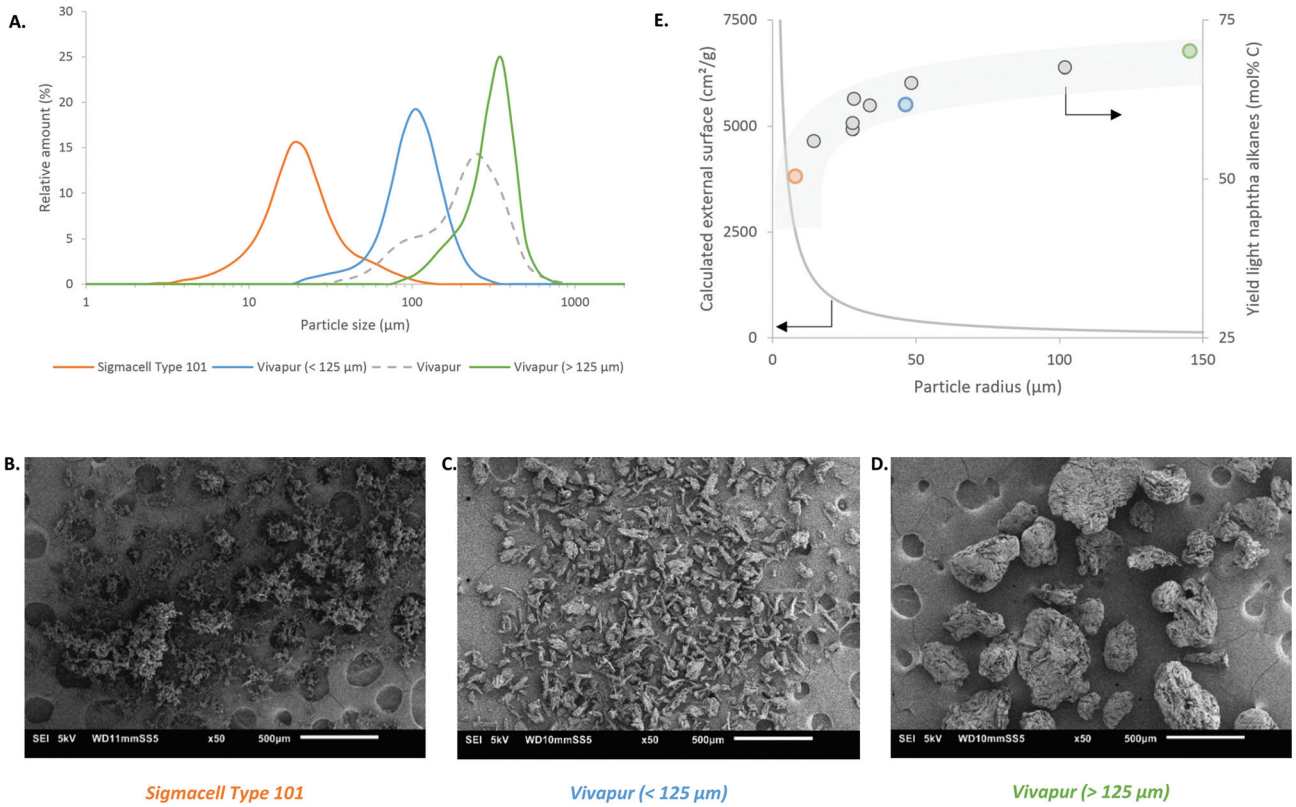

Fig. 2 Particle size distribution of the three cellulose substrates, measured with laser diffraction (A). SEM pictures of Sigmacell Type 101 (B); Vivapur (<125 µm) (C) and Vivapur (>125 µm) (D). Yield of light naphtha alkanes (E), starting from different cellulose substrates with Sigmacell Type 101, Vivapur (<125 µm) and Vivapur (>125 µm) highlighted. Improvement of the yield can be realized by using cellulose (2 g) with a bigger particle size. The highest improvements in yield (bullets) are seen, if the decrease in accessibility, external surface, is the highest. The colours mark the same substrates in all figures A–E.

purified cellulose fractions containing residual hemicellulose and lignin parts.[23,73–77]

Three cellulose pulps with a small amount of impurities were tested to address the impact of cellulose purity: α-cellulose, still containing some hemicellulose; wheat straw organosolv pulp containing both hemicellulose and lignin; and the bleached version of the latter. Their composition and the corresponding light naphtha yield are found in Table 2. To evaluate the efficiency of the catalytic system in the presence of impurities, the yield of C_6 alkanes (mainly methylcyclopentane and *n*-hexane) should be considered, as they originate from C_6 sugars, and thus mainly from cellulose. In addition, Whatman filter 4, which is from a physical point of view similar to authentic highly dense cellulose fibers in a lignocellulosic matrix, is chosen as benchmark. The similar C_6 alkane yields (in Table 2) for the different celluloses suggest that the presence of impurities has no influence on the efficiency of cellulose-to-naphtha reactions (Table 2, entries 1–4). Moreover, the mild pretreatment procedures, which partly removed hemicellulose and lignin fractions, keep intact the original and dense cellulose structure, which is very interesting for the catalytic system under study here considering our findings regarding the impact of the cellulose external surface. While the efficiency of cellulose conversion is almost constant, the total yield of light naphtha is lower compared to that from pure cellulose substrates. This decrease is caused by the inefficient conversion of hemicellulose (mainly C_5 sugars) and lignin under the applied reaction circumstances. Though these impurities do not affect the cellulose-to-naphtha reaction, their conversion to light naphtha alkanes is less efficient and therefore their presence in the cellulosic feedstock should be minimized (Table 2, entries 1–4). If their valorisation is pursued for instance for economic reasons, their fractionation will thus be a prerequisite.

For the hemicellulose fraction, the current conditions are likely too harsh to convert these amorphous and branched sugar polymers selectively into alkanes. Tomishige *et al.* noticed the same issue and reported the formation of humins as major drawback.[78] Recent work by Ennaert *et al.* also warned for the use of unbalanced bifunctional (metal-acidic) catalytic systems for hemicellulose conversion to pentitols.[79] Moreover, the acidic condition, required to convert the crystalline rigid celluloses, chemically transforms lignin through acid-catalysed condensation into (usually larger and) stable lignin derivatives, which may foul the catalyst sites.[76,80,81] Therefore, in order to efficiently valorise the complete lignocellulosic biomass, a multistep process, which involves practical fractionation of the individual lignocellulose constituents,

Table 2 HDO of different raw (ligno)cellulosic feedstocks[a]

Entry	Substrate[f]	Composition[b] (wt%)				Yield from C_6 sugars (%)		Total yield[d] (%)
		C_6 sugars	C_5 sugars	Lignin	Others[c]	*n*-Hex	Other C_6 alkanes[e]	Light naphtha
1	Whatman filter 4	100	—	—	—	49	9	68
2	α-Cellulose	83	17	—	—	48	8	54
3	Wheat straw organosolv	70	8	16	6	45	12	45
4	Wheat straw organosolv bleached	74	3	6	16	42	8	51

[a] Conditions: 2 g substrate; 4.8 g TSA; 0.25 g htTSA(2)Ru/C; biphasic system: water/*n*-decane (30 : 10); 50 bar H_2 at RT; temperature programme: RT to 423 K (±12 K min^{-1}) and from 423 K to 493 K (±0.5 K min^{-1}); total reaction time of 5 h. [b] Ennaert *et al.* recently published the composition of the respective substrates.[23] [c] Others: sum of ash; proteins; acetyl; uronic acids and extractives. [d] The total yield is based on the amount of carbon coming from C_5 sugars, C_6 sugars and lignin. [e] Other C_6 alkanes: 2-methylpentane; 3-methylpentane; methylcyclopentane and cyclohexane. [f] Characterization data is available in section B of the ESI.

viz. cellulose, hemicellulose and lignin, followed by their individual chemical conversion, is highly advised. This strategy will lead to the most effective biorefinery, since the processing conditions can be optimised to the needs of each fraction. Whereas most fractionation processes focus on the isolation of one purified fraction, usually cellulose, more recent initiatives attempts to refine the biomass with regard to produce two or three separate fractions. Selective removal of lignin with formation of a fairly pure and easily processable sugar pulp was recently introduced in the lignin-first processing of lignocellulose,[82–89] but also other initiatives are under development.[90] Lignin-first technology in presence of small quantities of H_3PO_4 is perhaps the most notable one. This technology generates a purified cellulose pulp from woody biomass, besides a solution containing a soluble lignin oil and methyl sugars from the hemicellulose fraction.[91]

Closed energy and mass balances

There are many ways to assess the viability and sustainability of a biorefinery as multiple factors such as feedstock cultivation, biomass transportation, process efficiency and product added-value are involved. Moreover, these parameters are influenced by specific boundary conditions (*e.g.* biomass density in the surrounding area and infrastructure for transportation).[92,93] By consequence, concepts such as net atmospheric carbon ration (NACR) and indirect land use change emissions (ILUC) are important parameters to evaluate the entire life cycle of each process from a sustainable point of view.[94–98] The most important stumbling blocks associated with biorefineries are the following: feedstock price, food competition, loss of biodiversity, additional emissions through the replacement of wood and grassland in new cropland, new infrastructure needs, *etc*. The present LPCtoN technology may be considered as a potential second generation biomass-to-liquid process replacing crude oil to reach the government-imposed renewable end-objectives.[99,100] It creates a drop-in light naphtha from non-edible lignocellulose feedstock, ideally from waste or fast-growing trees (*e.g.* poplar and willow) from sustainably managed forests. However, implementation of such processes is only realistic within a certain framework, *e.g.* for making additives for the large fuel markets in expectation of electrification or, more likely, as valuable alternative in the smaller markets of chemicals and materials.[1] Moreover, large quantities of hydrogen are consumed and therefore the self-sustainability (with regard to carbon, hydrogen and energy neutrality) may be argued.

Beside use of renewable (ligno)cellulose, one should also be able to realize an integrated biorefinery with a closed-loop of mass and energy. Recent biofactories, in which chemicals are produced from renewable resources and solar energy is used to co-valorise CO_2, have been discussed, but also integration of petrochemistry and solar has been suggested. Centi *et al.* recently introduced the concept of the biofactory, taking into account the whole production process by integration of renewable energy (*e.g.* solar) and valorisation of CO_2.[101–103] Also, Jacobs *et al.* proposed a conceptual biorefinery, merging petroleum and solar refineries.[104] The generation of CO_2, *e.g.* to be considered as the end-of-life of most hydrocarbon chemicals, but also the result of H_2 generation from carbon containing resources, can be seen as looped by photosynthesis during lignocellulosic plant growth, and may be largely regarded as carbon neutral as long as renewable resources were used. Natural or artificial techniques, requiring a limited input of energy (*e.g.* solar), could be used in the long term here to convert such spent carbon into working carbon.[105,106]

Sustainable production of hydrogen in the biorefinery is an important challenge. Today, most H_2 is produced through steam-reforming of (shale) natural gas, while in light of a 100% renewability criterion, a non-fossil resource is required. Though economically sound on a short term to initiate biorefinery activities, the search for and the integration of other techniques such as biological hydrogen production,[107] photocatalytic splitting of water,[108–111] gasification of biomass,[112] aqueous-phase-reforming (APR)[113–117] and steam-reforming[118,119] of biomass derived gaseous products should be considered to offer more sustainable opportunities on the long term, but they are still in their infancy at the commercial scale. In addition to APR and steam-reforming, there might be a third and fourth option to recuperate additional hydrogen, which is particularly valid for the presented LPCtoN technology: steam or catalytic cracking of *n*-hexane to short olefins[27,28] and dehydrocyclisation of *n*-hexane (and the other cyclic C_6 alkanes) to

benzene.[29–31] The latter is in particular interesting since the technology could lead to the on-purpose production of bio-benzene. The cyclisation to benzene, producing hydrogen gas, for instance described in presence of Pt–Ba loaded L zeolite at 773 K,[29–31,120] may pave the way to the production of bio-based ethylbenzene and styrene. Other aromatics such as phenols and anilines will more likely be targeted starting from the lignin (oil) fraction.[121–124] In section D of the ESI† a short case study, with respect to the typical capacity of a biorefinery, illustrates the feasibility of synthesizing such renewable chemicals and materials.

Though highly relevant in general, evaluating the above issues is very complex. Therefore, rather than focussing already on the complete life cycle analysis of the proposed biorefinery, this contributions wants to discuss the sustainability at the technical level, with regard to carbon and hydrogen neutrality of a potential stand-alone process.

In what follows, we will conceptually close mass and energy balances for an integrated LPCtoN process, and give suggestions for the carbon and hydrogen neutral production of the renewable alkanes and thereof derived bio-benzene. First, this exercise is done taking into account two scenarios, one which includes only reforming for hydrogen recuperation and a second one, which includes both reforming and dehydrocyclisation. The scenarios are illustrated in Fig. 3. Before evaluating the two scenarios for the real situation (see later), the different process streams were calculated in thermodynamic equilibrium using Aspen Tech 7.3 software assuming no net production/consumption of hydrogen in the process. Rather than directly using the precise (waste) products available in the LPCtoN process, obvious model molecules to produce hydrogen were selected. The calculations used therefore *n*-hexane (as a model of potential waste alkanes) for steam-reforming, ethylene glycol (as a model of polyol waste) for APR and *n*-hexane for the dehydrocyclisation to benzene. Note that the water gas shift reaction is taken into account in the steam-reforming process as to maximize the potential hydrogen production. Details of the calculations are presented in the ESI (section E in the ESI†). The thermodynamic data and the calculated streams for the specific case of the combination of reforming of *n*-hexane (here by steam) and dehydrocyclisation are illustrated in Table 3 and Fig. 4.

Three main conclusions emerge from these calculations. Firstly, the carbon efficiency of the overall process depends strongly on the envisioned end product, showing a value of 63.2% and 80.0% for *n*-hexane and benzene, respectively. The latter number indicates that the overall production of two benzene molecules is accompanied with the formation of three bio-derived CO_2 molecules, which will enter the photosynthesis cycle to reform cellulose using sun light input. Secondly, there is no additional energy requirement to obtain the above mentioned reaction outcomes, because the energy release during cellulose-to-hexane processing overcompensates the endothermicity of the reforming and dehydrocyclisation

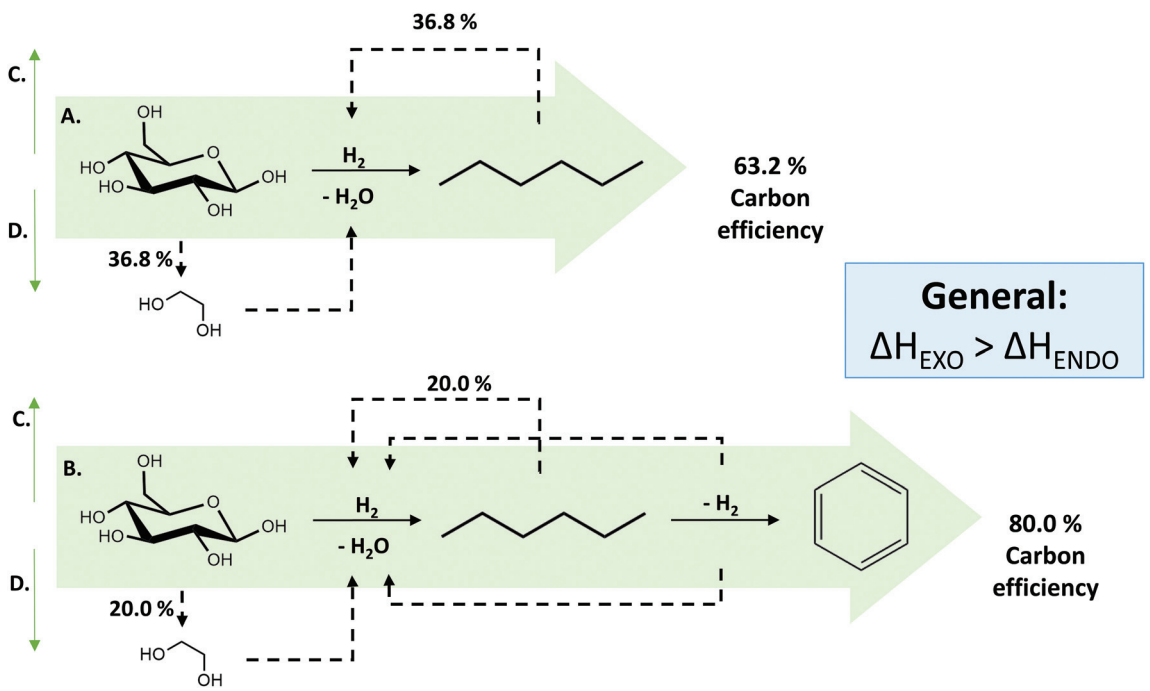

Fig. 3 Overview of the 2 scenarios to generate end products (*n*-hexane or benzene) with 100% renewable carbon and hydrogen. The amount of carbon used for H_2 recovery is based on equal consumption and production of H_2 for 100% efficient reactions. The thermodynamics are calculated at the most common reactions conditions by using AspenTech 7.3 software. Different reactions are HDO of glucose to *n*-hexane (A); HDO of glucose to *n*-hexane and subsequently dehydrocyclisation to benzene (B); steam-reforming of *n*-hexane (C) and production of ethylene glycol form sugars and subsequently APR (D).

Table 3 Calculated streams (thermodynamic equilibrium) of combined HDO of glucose, dehydrocyclisation of *n*-hexane and steam-reforming of *n*-hexane

	HDO of glucose[a]			Dehydrocyclisation of *n*-hexane[b]		Steam-reforming of *n*-hexane[c]	
Component	Mixed[d]	Vapor[e]	Liquid[e]	Vapor[d]	Vapor[e]	Vapor[d]	Vapor[e]
$C_6H_{12}O_6$ (mol h^{-1})	5.0	1.2×10^{-8}	1.2×10^{-3}	0	0	0	0
H_2 (mol h^{-1})	35.0	8.1×10^{-3}	1.3×10^{-4}	0	12.4	0	18.2
C_6H_{14} (mol h^{-1})	0	5.0	1.9×10^{-2}	4.0	1.0	1.0	4.1×10^{-2}
H_2O (mol h^{-1})	0	2.8	27.2	0	0	12.0	4.9×10^{-1}
C_6H_6 (mol h^{-1})	0	0	0	0	3.1	0	0
CO_2 (mol h^{-1})	0	0	0	0	0	0	5.8
Total (mol h^{-1})	40.0	7.7	27.3	4.0	16.5	13.0	24.5
Molar H (kJ mol^{-1})	-1.4×10^{2}	-1.7×10^{2}	-2.7×10^{2}	-6.0×10^{1}	3.5×10^{1}	-1.9×10^{2}	-7.1×10^{1}
Molar S (kJ mol^{-1} K^{-1})	-1.3×10^{-1}	-3.4×10^{-1}	-1.2×10^{-1}	-3.8×10^{-1}	-2.0×10^{-2}	-3.4×10^{-2}	2.9×10^{-2}
ΔH (kJ h^{-1})		−2948.0		815.6		782.6	

Conditions: [a] T = 493 K; p = 65 bar. [b] T = 773 K; p = 10 bar. [c] T = 1073 K; p = 10 bar. [d] Starting mixture and input in AspenTech software. [e] End streams.

reaction. Our examples show an excess of 300 kJ mol^{-1} (per mol glucose converted), which may well be used to support other unit operations such as separation. Thirdly, considering the end-of-life of the products, burning of the products ultimately delivers a CO_2 to water molar ratio of unity, which enters the photosynthesis cycle regenerating cellulose. Though not yet mature, also artificial techniques can (partially) be used to valorise the amount of released CO_2 in the long term, *e.g.* using the excess of released energy or sun light.[105,106]

Similar calculations were performed using the real product outcome of an experimental cellulose-to-naphtha reaction. We have selected the data of Vivapur cellulose processing (Table 1,

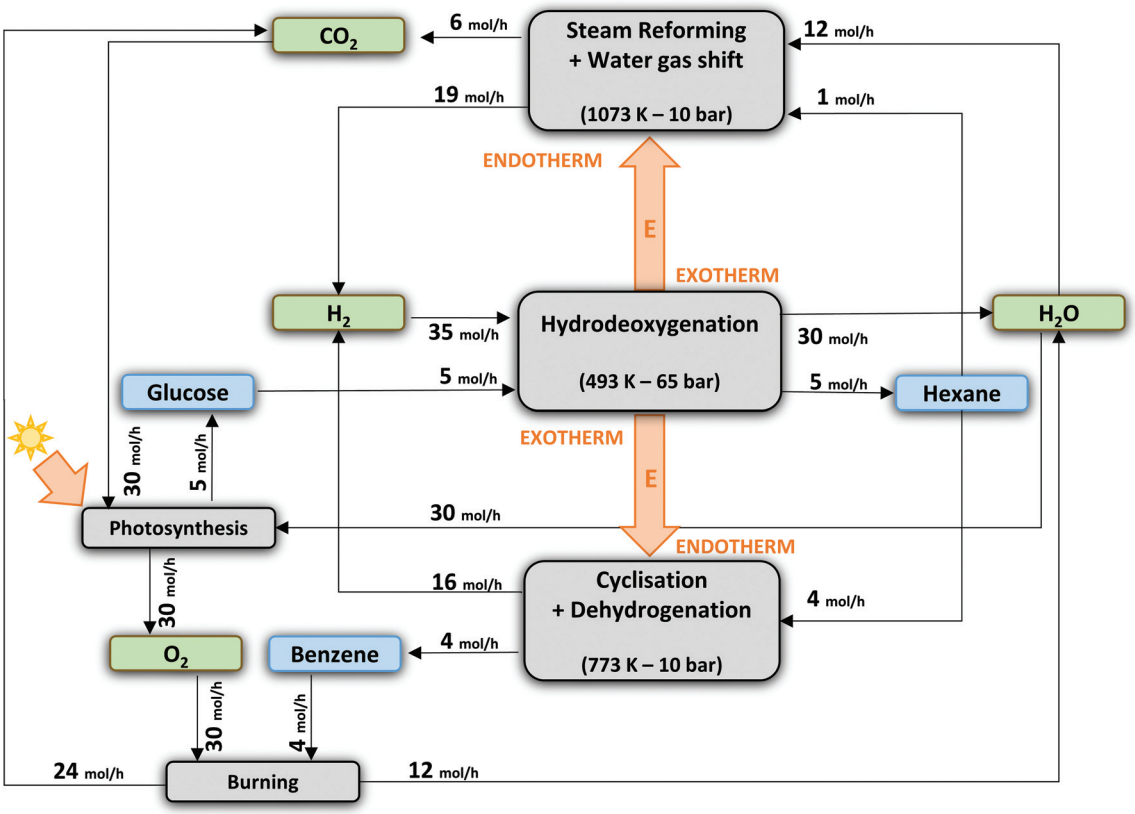

Fig. 4 Theoretical process scheme assuming 100 mol% C of *n*-hexane yield (of which 1/5 is steam-reformed for H_2-recuperation) and 80 mol% C of benzene yield.

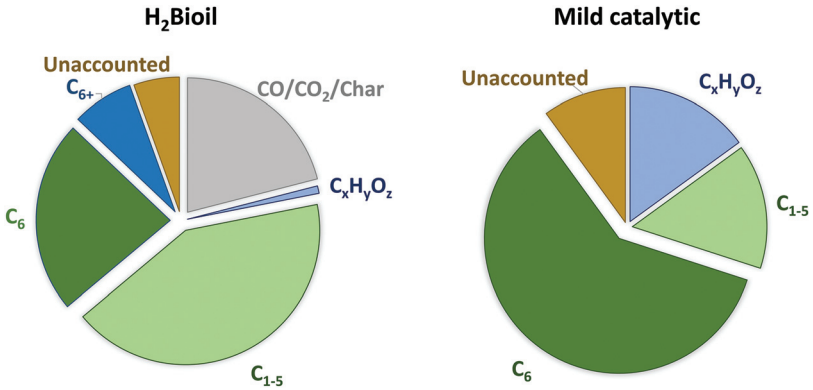

Fig. 5 Product distributions (mol% C) for the H_2Bioil process (consecutive two-step process of fast-hydropyrolysis and downstream vapor-phase catalytic hydrodeoxygenation)[41] and the here described mild catalytic one-pot process (hydrodeoxygenation) from the experiments with cellulose.

entry 10), as this feedstock produces the highest C_6 alkane yield, approaching 60 mol% C, consisting of 86% *n*-hexane, 2% methylpentanes, 3% cyclohexane and 9% methylcyclopentane. The total content of light hydrocarbons, almost exclusively straight, shorter alkanes ($C_{<6}$) amounts to 15 mol% C, consisting of 74% C_5, 7% C_4 and 19% C_1, while the aqueous phase contains about 15 mol% C oxygenates such as hexitols and other polyols. The deficiency in mass balance, about 10 mol% C, is because of unknowns. The product distribution is seen in Fig. 5 (right). These data show that, in contrast to a large production of lights such as in fast-hydropyrolysis, a more selective production of C_6 alkanes is realized. While pyrolysis is useful to obtain a mixture of gaseous hydrocarbons, the two-phase liquid catalytic strategy with Ru/C and tungstate heteropolyacids is more appropriate for chemical applications. The hydrogen consumption of both

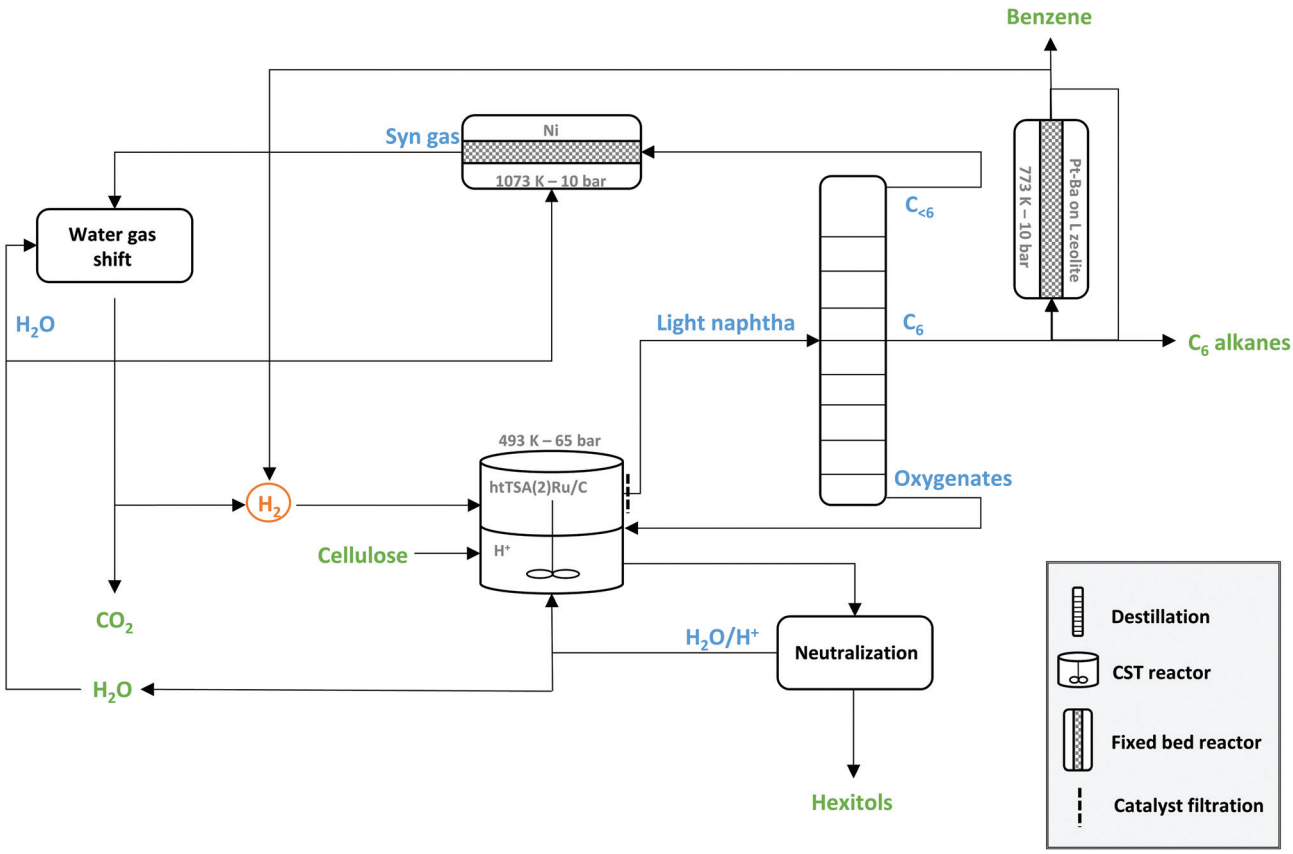

Fig. 6 Biorefinery scenario for the conversion of cellulose into *n*-hexane, benzene and hextiol-derived products, with additional strategies toward closed mass and energy streams. Compounds presented in green and blue are end-products and intermediate products, respectively.

processes is very similar and amounts to roughly 0.05 kg H_2 per kg of dry cellulose feed.

Hydrogen can be recovered from both light gas $C_{<6}$ mixture as well as from the organic waste in the aqueous phase. Steam-reforming of the first waste stream foresees about 57% of the consumed hydrogen. An additional reforming of the aqueous waste, either through aqueous or steam-reforming reactions, led to almost 80% of the required hydrogen. This scenario indicates a hydrogen shortness, pointing out that an additional dehydrocyclisation of the C_6 fraction is a nice option to fill the hydrogen gap. A 50% conversion of the C_6 fraction to benzene is sufficient to balance the hydrogen in the overall process. Full details of the calculations can be found in section F of the ESI.†

If benzene is the desired product in the biorefinery, 43% of hydrogen may be recuperated through dehydrocyclisation. Steam-reforming of the light gaseous fraction provides the remaining hydrogen. This scenario fulfils a 100% renewable hydrogen LPCtoN biorefinery (section F in the ESI†). Ideally, two out of ten carbons of cellulose should end up in the light gas waste to foresee the hydrogen, the remaining of the carbons ultimately ending in benzene. A stand-alone LPCtoN biorefinery thus should not necessary operate exclusively towards one specific product, as the remaining waste is usefully recuperated into renewable hydrogen streams. A possible process scheme for such a closed-loop (stand-alone) biorefinery is illustrated in Fig. 6, showing the central cellulose-to-naphtha unit, combined with benzene formation, and the hydrogen recuperation units.

Conclusions

The presented LPCtoN biorefinery can be an interesting opportunity to selectively produce bio-derived light naphtha alkanes, and more specifically C_6 alkanes, and as such it may gradually fuel the existing naphtha facilities with bio-derived carbon. Two key points of the biorefinery were addressed here: (i) structural and compositional aspects of the cellulose biomass, and (ii) the renewable origin (or not) of hydrogen. Perhaps somewhat surprising, this study reveals the highest alkane yields from large-sized fibrous crystalline cellulose. The rationale is to keep cellulose hydrolysis the slowest step as to protect the reactive sugar molecules in the cellulose structure. A too fast release of reactive sugars in solution otherwise results in side-reactions producing for instance humins. Therefore costly mechanical or other treatments to lower cellulose crystallinity are not necessary. Also interesting to notice, presence of hemicellulose and lignin impurities also preserves the catalytic outcome of the LPCtoN process. As they are hardly converted to alkanes, but rather end-up in an oligomeric waste stream, a rough cellulose purification step is advised. The separated hemicellulose and lignin fractions may be better used in other valorisation processes. From economic point of view, the ability of directly processing large and impure cellulose fibres obviates the need of a series of costly pretreatment steps in the overall process.

Sustainable biorefinery schemes should attempt not only to use a renewable feedstock such as lignocellulose, but also other reagents such as hydrogen should preferably be renewable. The issue of renewable hydrogen is countered here by integrating hydrogen producing technologies like reforming and dehydrocyclisation. Both mass and energy balances prove the viability of a stand-alone biorefinery for making *n*-hexane and benzene. In the first case, reforming of different side streams is required, while in the benzene case, reforming of only the light hydrocarbon gases ($C_{<6}$ fraction) is already sufficient to foresee hydrogen. Considering a hydrogen neutral process, 59% of renewable benzene, *e.g.* for styrene and aniline production, can be technically produced with excess of process energy (300 kJ per mol glucose converted), available to the other unit operations. In the end, a completely self-supporting biorefinery process is put forward using solar energy in form of biomass production as the only input to produce useful drop-in chemicals. Research is ongoing to make a more complete life cycle analysis of the integrated process taking into account net atmospheric carbon ratios and indirect land use change emissions.

Acknowledgements

This work was performed in the framework of IWT-SBO project ARBOREF. A. D. and T. E. acknowledge the Agency for Innovation by Science and Technology (IWT) for a Ph.D. grant. J. V. thanks the Flemish Institute for Technological Research (VITO) for a doctoral fellowship. M. D. acknowledge Research Foundation-Flanders (FWO) for financial support. The authors kindly thank Arjan T. Smit, Wouter J. J. Huijgen and Annick Vanhulsel for respectively providing the organosolv samples and use of DLS equipment.

Notes and references

1 A. Deneyer, T. Renders, J. Van Aelst, S. Van den Bosch, D. Gabriëls and B. F. Sels, *Curr. Opin. Chem. Biol.*, 2015, **29**, 40–48.
2 A. J. Ragauskas, C. K. Williams, B. H. Davison, G. Britovsek, J. Cairney, C. A. Eckert, W. J. Frederick, J. P. Hallett, D. J. Leak, C. L. Liotta, J. R. Mielenz, R. Murphy, R. Templer and T. Tschaplinski, *Science*, 2006, **311**, 484–489.
3 G. W. Huber, S. Iborra and A. Corma, *Chem. Rev.*, 2006, **106**, 4044–4098.
4 D. M. Alonso, J. Q. Bond and J. A. Dumesic, *Green Chem.*, 2010, **12**, 1493–1513.
5 A. Corma, S. Iborra and A. Velty, *Chem. Rev.*, 2007, **107**, 2411–2502.
6 M. J. Climent, A. Corma and S. Iborra, *Green Chem.*, 2014, **16**, 516–547.

7 J. A. Geboers, S. Van de Vyver, R. Ooms, B. Op de Beeck, P. A. Jacobs and B. F. Sels, *Catal. Sci. Technol.*, 2011, **1**, 714–726.
8 S. Van de Vyver, J. Geboers, P. A. Jacobs and B. F. Sels, *ChemCatChem*, 2011, **3**, 82–94.
9 P. Gallezot, *Chem. Soc. Rev.*, 2012, **41**, 1538–1558.
10 R. A. Sheldon, *Green Chem.*, 2014, **16**, 950–963.
11 J. C. Serrano-Ruiz, R. M. West and J. A. Dumesic, *Annu. Rev. Chem. Biomol. Eng.*, 2010, **1**, 79–100.
12 J. C. Serrano-Ruiz, R. Luque and A. Sepúlveda-Escribano, *Chem. Soc. Rev.*, 2011, **40**, 5266–5281.
13 J. C. Serrano-Ruiz and J. A. Dumesic, *Energy Environ. Sci.*, 2011, **4**, 83–99.
14 T. Ennaert, J. Van Aelst, J. Dijkmans, R. De Clercq, W. Schutyser, M. Dusselier, D. Verboekend and B. F. Sels, *Chem. Soc. Rev.*, 2016, **45**, 584–611.
15 M. Dusselier, M. Mascal and B. Sels, in *Selective Catalysis for Renewable Feedstocks and Chemicals*, ed. K. M. Nicholas, Springer International Publishing, 2014, ch. 544, vol. 353, pp. 1–40.
16 M. Dusselier, P. Van Wouwe, A. Dewaele, P. A. Jacobs and B. F. Sels, *Science*, 2015, **349**, 78–80.
17 R. De Clercq, M. Dusselier, C. Christiaens, J. Dijkmans, R. I. Iacobescu, Y. Pontikes and B. F. Sels, *ACS Catal.*, 2015, **5**, 5803–5811.
18 T. Wang, M. W. Nolte and B. H. Shanks, *Green Chem.*, 2014, **16**, 548–572.
19 J. A. Dumesic, Y. J. Pagán-Torres, T. Wang and B. H. Shanks, *US* 8642791B2, 2014.
20 J. A. Dumesic, S. G. Wettstein, D. M. Alonso and E. I. Gurbuz, *US* 8962856B2, 2015.
21 S. G. Wettstein, D. M. Alonso, Y. Chong and J. A. Dumesic, *Energy Environ. Sci.*, 2012, **5**, 8199–8203.
22 R. Weingarten, W. C. Conner and G. W. Huber, *Energy Environ. Sci.*, 2012, **5**, 7559–7574.
23 T. Ennaert, B. Op de Beeck, J. Vanneste, A. T. Smit, W. J. J. Huijgen, A. Vanhulsel, P. A. Jacobs and B. F. Sels, *Green Chem.*, 2016, **18**, 2095–2105.
24 H. Kobayashi and A. Fukuoka, *Green Chem.*, 2013, **15**, 1740–1763.
25 M. Yabushita, H. Kobayashi and A. Fukuoka, *Appl. Catal., B*, 2014, **145**, 1–9.
26 M. R. Rahimpour, M. Jafari and D. Iranshahi, *Appl. Energy*, 2013, **109**, 79–93.
27 N. Rahimi and R. Karimzadeh, *Appl. Catal., A*, 2011, **398**, 1–17.
28 K. M. Van Geem, M.-F. Reyniers, G. B. Marin, J. Song, W. H. Green and D. M. Matheu, *AIChE J.*, 2006, **52**, 718–730.
29 W. C. Buss and T. R. Hughes, *US* 4435283A, 1984.
30 P. Mériaudeau and C. Naccache, *Catal. Rev.*, 1997, **39**, 5–48.
31 C. T. O'Connor, in *Handbook of Heterogeneous Catalysis*, ed. G. Ertl, H. Knözinger and J. Weitkamp, 2008, vol. 1, pp. 3123–3133.
32 M. L. Campbell, *Ullmann's Encycl. Ind. Chem.*, 2012, 673–710.
33 M. Dugal, G. Sankar, R. Raja and J. M. Thomas, *Angew. Chem., Int. Ed.*, 2000, **39**, 2310–2313.
34 R. C. Baliban, J. A. Elia and C. A. Floudas, *Ind. Eng. Chem. Res.*, 2013, **52**, 3381–3406.
35 S. D. Phillips, J. K. Tarud, M. J. Biddy and A. Dutta, *Gasoline from Wood via Integrated Gasification, Synthesis, and Methanol-to- Gasoline Technologies*, 2011.
36 U. Olsbye, S. Svelle, M. Bjørgen, P. Beato, T. V. W. Janssens, F. Joensen, S. Bordiga and K. P. Lillerud, *Angew. Chem., Int. Ed.*, 2012, **51**, 5810–5831.
37 H. Jahangiri, J. Bennett, P. Mahjoubi, K. Wilson and S. Gu, *Catal. Sci. Technol.*, 2014, **4**, 2210–2229.
38 S. Wang, Q. Yin, J. Guo, B. Ru and L. Zhu, *Fuel*, 2013, **108**, 597–603.
39 M. Dalil, M. Sohrabi and S. J. Royaee, *J. Ind. Eng. Chem.*, 2012, **18**, 690–696.
40 A. V. Bridgwater, *Biomass Bioenergy*, 2012, **38**, 68–94.
41 V. K. Venkatakrishnan, W. N. Delgass, F. H. Ribeiro and R. Agrawal, *Green Chem.*, 2015, **17**, 178–183.
42 N. R. Singh, D. S. Mallapragada, R. Agrawal and W. E. Tyner, *Biomass Convers. Biorefin.*, 2012, **2**, 141–148.
43 N. R. Singh, W. N. Delgass, F. H. Ribeiro and R. Agrawal, *Environ. Sci. Technol.*, 2010, **44**, 5298–5305.
44 A. Corma, O. de la Torre and M. Renz, *Energy Environ. Sci.*, 2012, **5**, 6328–6344.
45 D. M. Alonso, S. G. Wettstein and J. A. Dumesic, *Green Chem.*, 2013, **15**, 584–595.
46 H. Olcay, A. V. Subrahmanyam, R. Xing, J. Lajoie, J. A. Dumesic and G. W. Huber, *Energy Environ. Sci.*, 2013, **6**, 205–216.
47 J. Q. Bond, A. A. Upadhye, H. Olcay, G. A. Tompsett, J. Jae, R. Xing, D. M. Alonso, D. Wang, T. Zhang, R. Kumar, A. Foster, S. M. Sen, C. T. Maravelias, R. Malina, S. R. H. Barrett, R. Lobo, C. E. Wyman, J. A. Dumesic and G. W. Huber, *Energy Environ. Sci.*, 2014, **7**, 1500–1523.
48 J. Xin, S. Zhang, D. Yan, O. Ayodele, X. Lu and J. Wang, *Green Chem.*, 2014, **16**, 3589–3595.
49 D. Liu and E. Y. X. Chen, *ACS Catal.*, 2014, **4**, 1302–1310.
50 J. Yang, N. Li, G. Li, W. Wang, A. Wang, X. Wang, Y. Cong and T. Zhang, *Chem. Commun.*, 2014, **50**, 2572–2574.
51 Y. Nakagawa, S. Liu, M. Tamura and K. Tomishige, *ChemSusChem*, 2015, **8**, 1114–1132.
52 E. R. Sacia, M. H. Deaner, Y. Louie and A. T. Bell, *Green Chem.*, 2015, **17**, 2393–2397.
53 S. Liu, M. Tamura, Y. Nakagawa and K. Tomishige, *ACS Sustainable Chem. Eng.*, 2014, **2**, 1819–1827.
54 Y. Liu, L. Chen, T. Wang, X. Zhang, J. Long, Q. Zhang and L. Ma, *RSC Adv.*, 2015, **5**, 11649–11657.
55 B. Op de Beeck, M. Dusselier, J. Geboers, J. Holsbeek, E. Morré, S. Oswald, L. Giebeler and B. F. Sels, *Energy Environ. Sci.*, 2015, **8**, 230–240.
56 Y. Liu, L. Chen, T. Wang, Q. Zhang, C. Wang, J. Yan and L. Ma, *ACS Sustainable Chem. Eng.*, 2015, **3**, 1745–1755.
57 F. Cherubini, *Energy Convers. Manage.*, 2010, **51**, 1412–1421.

58 L. Segal, J. J. Creely, A. E. Martin and C. M. Conrad, *Text. Res. J.*, 1959, **29**, 786–794.
59 M. Benoit, A. Rodrigues, K. De Oliveira Vigier, E. Fourré, J. Barrault, J.-M. Tatibouët and F. Jérôme, *Green Chem.*, 2012, **14**, 2212–2215.
60 F. Jérôme, G. Chatel and K. De Oliveira Vigier, *Green Chem.*, 2016, **18**, 3903–3913.
61 M. Sasaki, B. Kabyemela, R. Malaluan, S. Hirose, N. Takeda, T. Adschiri and K. Arai, *J. Supercrit. Fluids*, 1998, **13**, 261–268.
62 S. A. Maurer, C. N. Bedbrook and C. J. Radke, *Ind. Eng. Chem. Res.*, 2012, **51**, 11389–11400.
63 S. K. R. Patil and C. R. F. Lund, *Energy Fuels*, 2011, **25**, 4745–4755.
64 S. J. Dee and A. T. Bell, *ChemSusChem*, 2011, **4**, 1166–1173.
65 R. Ooms, M. Dusselier, J. A. Geboers, B. Op de Beeck, R. Verhaeven, E. Gobechiya, J. A. Martens, A. Redl and B. F. Sels, *Green Chem.*, 2014, **16**, 695–707.
66 G. Zhao, M. Zheng, J. Zhang, A. Wang and T. Zhang, *Ind. Eng. Chem. Res.*, 2013, **52**, 9566–9572.
67 N. Mosier, C. Wyman, B. Dale, R. Elander, Y. Y. Lee, M. Holtzapple and M. Ladisch, *Bioresour. Technol.*, 2005, **96**, 673–686.
68 Q. Zhang and F. Jérôme, *ChemSusChem*, 2013, **6**, 2042–2044.
69 F. Boissou, N. Sayoud, K. De Oliveira Vigier, A. Barakat, S. Marinkovic, B. Estrine and F. Jérôme, *ChemSusChem*, 2015, **8**, 3263–3269.
70 H. Krässig, J. Schurz, R. G. Steadman, K. Schliefer, W. Albrecht, M. Mohring and H. Schlosser, *Ullmann's Encycl. Ind. Chem.*, 2012, **6**, 279–332.
71 M. Ragnar, G. Henriksson, M. E. Lindström, M. Wimby, J. Blechschmidt and S. Heinemann, *Ullmann's Encycl. Ind. Chem.*, 2014, **6**, 3–92.
72 G. E. Reier, Avicel PH Microcrystalline Cellulose, *NF, Ph Eur., JP, BP*, 2000, pp. 1–27.
73 W. J. J. Huijgen, A. T. Smit, J. H. Reith and H. Den Uil, *J. Chem. Technol. Biotechnol.*, 2011, **86**, 1428–1438.
74 W. J. J. Huijgen, A. T. Smit, P. J. de Wild and H. den Uil, *Bioresour. Technol.*, 2012, **114**, 389–398.
75 W. J. J. Huijgen, J. H. Reith and H. Den Uil, *Ind. Eng. Chem. Res.*, 2010, **49**, 10132–10140.
76 J. Wildschut, A. T. Smit, J. H. Reith and W. J. J. Huijgen, *Bioresour. Technol.*, 2013, **135**, 58–66.
77 X. Pan, C. Arato, N. Gilkes, D. Gregg, W. Mabee, K. Pye, Z. Xiao, X. Zhang and J. Saddler, *Biotechnol. Bioeng.*, 2005, **90**, 473–481.
78 S. Liu, Y. Okuyama, M. Tamura, Y. Nakagawa, A. Imai and K. Tomishige, *Green Chem.*, 2016, **18**, 165–175.
79 T. Ennaert, S. Feys, D. Hendrikx, P. A. Jacobs and B. F. Sels, *Green Chem.*, 2016, DOI: 10.1039/C6GC01439A.
80 R. El Hage, N. Brosse, P. Sannigrahi and A. Ragauskas, *Polym. Degrad. Stab.*, 2010, **95**, 997–1003.
81 S. Bauer, H. Sorek, V. D. Mitchell, A. B. Ibáñez and D. E. Wemmer, *J. Agric. Food Chem.*, 2012, **60**, 8203–8212.
82 S. Van den Bosch, W. Schutyser, R. Vanholme, T. Driessen, S.-F. Koelewijn, T. Renders, B. De Meester, W. J. J. Huijgen, W. Dehaen, C. M. Courtin, B. Lagrain, W. Boerjan and B. F. Sels, *Energy Environ. Sci.*, 2015, **8**, 1748–1763.
83 S. Van den Bosch, W. Schutyser, S.-F. Koelewijn, T. Renders, C. M. Courtin and B. F. Sels, *Chem. Commun.*, 2015, **51**, 13158–13161.
84 W. Schutyser, S. Van den Bosch, T. Renders, T. De Boe, S.-F. Koelewijn, A. Dewaele, T. Ennaert, O. Verkinderen, B. Goderis, C. M. Courtin and B. F. Sels, *Green Chem.*, 2015, **17**, 5035–5045.
85 M. V. Galkin and J. S. M. Samec, *ChemSusChem*, 2014, **7**, 2154–2158.
86 P. Ferrini and R. Rinaldi, *Angew. Chem., Int. Ed.*, 2014, **53**, 8634–8639.
87 T. Parsell, S. Yohe, J. Degenstein, T. Jarrell, I. Klein, E. Gencer, B. Hewetson, M. Hurt, J. I. Kim, H. Choudhari, B. Saha, R. Meilan, N. Mosier, F. Ribeiro, W. N. Delgass, C. Chapple, H. I. Kenttämaa, R. Agrawal and M. M. Abu-Omar, *Green Chem.*, 2015, **17**, 1492–1499.
88 Q. Song, F. Wang, J. Cai, Y. Wang, J. Zhang, W. Yu and J. Xu, *Energy Environ. Sci.*, 2013, **6**, 994–1007.
89 M. V. Galkin and J. S. M. Samec, *ChemSusChem*, 2016, **9**, 1544–1558.
90 J. S. Luterbacher, A. Azarpira, A. H. Motagamwala, F. Lu, J. Ralph and J. A. Dumesic, *Energy Environ. Sci.*, 2015, **8**, 2657–2663.
91 T. Renders, W. Schutyser, S. Van den Bosch, S.-F. Koelewijn, T. Vangeel, C. M. Courtin and B. F. Sels, *ACS Catal.*, 2016, **6**, 2055–2066.
92 V. Balan, *Int. Scholarly Res. Not.*, 2014, **2014**, 1–31.
93 A. W. Bhutto, K. Qureshi, R. Abro, K. Harijan, Z. Zhao, A. A. Bazmi, T. Abbas and G. Yu, *RSC Adv.*, 2016, **6**, 32140–32170.
94 D. J. Garcia and F. You, *ACS Sustainable Chem. Eng.*, 2015, **3**, 1732–1744.
95 P. Havlík, U. A. Schneider, E. Schmid, H. Böttcher, S. Fritz, R. Skalský, K. Aoki, S. De Cara, G. Kindermann, F. Kraxner, S. Leduc, I. McCallum, A. Mosnier, T. Sauer and M. Obersteiner, *Energy Policy*, 2011, **39**, 5690–5702.
96 H. H. Khoo, W. L. Ee and V. Isoni, *Green Chem.*, 2016, **18**, 1912–1922.
97 R. J. Plevin, J. Beckman, A. A. Golub, J. Witcover and M. O'Hare, *Environ. Sci. Technol.*, 2015, **49**, 2656–2664.
98 T. Searchinger, R. Heimlich, R. A. Houghton, F. Dong, A. Elobeid, J. Fabiosa, S. Tokgoz, D. Hayes and T. Yu, *Science*, 2008, **319**, 1238–1240.
99 J. Murray and D. King, *Nature*, 2012, **481**, 433–435.
100 R. Mukhopadhyay, *Chem. Eng. News*, 2011, 10–15.
101 S. Abate, P. Lanzafame, S. Perathoner and G. Centi, *ChemSusChem*, 2015, **8**, 2854–2866.
102 P. Lanzafame, G. Centi and S. Perathoner, *Chem. Soc. Rev.*, 2014, **43**, 7562–7580.
103 S. Bensaid, G. Centi, E. Garrone, S. Perathoner and G. Saracco, *ChemSusChem*, 2012, **5**, 500–521.

104 P. A. Jacobs, M. Dusselier and B. F. Sels, *Angew. Chem., Int. Ed.*, 2014, **53**, 8621–8626.
105 M. Aresta, A. Dibenedetto and A. Angelini, *Chem. Rev.*, 2014, **114**, 1709–1742.
106 E. V. Kondratenko, G. Mul, J. Baltrusaitis, G. O. Larrazábal and J. Pérez-Ramírez, *Energy Environ. Sci.*, 2013, **6**, 3112–3135.
107 P. C. Hallenbeck, M. Abo-Hashesh and D. Ghosh, *Bioresour. Technol.*, 2012, **110**, 1–9.
108 K. Maeda, K. Teramura, D. Lu, T. Takata, N. Saito, Y. Inoue and K. Domen, *Nature*, 2006, **440**, 295–295.
109 K. Shimura and H. Yoshida, *Energy Environ. Sci.*, 2011, **4**, 2467–2481.
110 S. Y. Reece, J. A. Hamel, K. Sung, T. D. Jarvi, A. J. Esswein, J. J. H. Pijpers and D. G. Nocera, *Science*, 2011, **334**, 645–648.
111 J. Liu, Y. Liu, N. Liu, Y. Han, X. Zhang, H. Huang, Y. Lifshitz, S. Lee, J. Zhong and Z. Kang, *Science*, 2015, **347**, 970–974.
112 J. Dai, J. Saayman, J. R. Grace and N. Ellis, *Annu. Rev. Chem. Biomol. Eng.*, 2015, **6**, 77–99.
113 R. D. Cortright, R. R. Davda and J. A. Dumesic, *Nature*, 2002, **418**, 964–967.
114 J. N. Chheda, G. W. Huber and J. A. Dumesic, *Angew. Chem., Int. Ed.*, 2007, **46**, 7164–7183.
115 R. R. Davda, J. W. Shabaker, G. W. Huber, R. D. Cortright and J. A. Dumesic, *Appl. Catal., B*, 2005, **56**, 171–186.
116 G. W. Huber, J. W. Shabaker and J. A. Dumesic, *Science*, 2003, **300**, 2075–2077.
117 T. P. Vispute and G. W. Huber, *Green Chem.*, 2009, **11**, 1433–1445.
118 H. Jeong and M. Kang, *Appl. Catal., B*, 2010, **95**, 446–455.
119 B. T. Schädel, M. Duisberg and O. Deutschmann, *Catal. Today*, 2009, **142**, 42–51.
120 R. J. Davis and E. G. Derouane, *Nature*, 1991, **349**, 313–315.
121 D. Verboekend, Y. Liao, W. Schutyser and B. F. Sels, *Green Chem.*, 2015, **18**, 297–306.
122 J. S. Kruger, N. S. Cleveland, S. Zhang, R. Katahira, B. A. Black, G. M. Chupka, T. Lammens, P. G. Hamilton, M. J. Biddy and G. T. Beckham, *ACS Catal.*, 2016, **6**, 1316–1328.
123 Y. Ono and H. Ishida, *J. Catal.*, 1981, **72**, 121–128.
124 J. Ma, H. Wang, M. Sun, F. Yang, Z. Wu, D. Wang and L. Chen, *Bull. Korean Chem. Soc.*, 2012, **33**, 387–392.